

# A study of the Mg II 2796.34 Å emission line in late-type normal and RS CVn stars

D. Cardini<sup>1</sup>, A. Cassatella<sup>1,2</sup>, M. Badiali<sup>1</sup>, A. Altamore<sup>2</sup>, and M.-J. Fernández-Figueroa<sup>3</sup>

<sup>1</sup> Istituto di Astrofisica Spaziale e Fisica Cosmica, CNR, via del Fosso del Cavaliere 100, 00133 Roma, Italy

<sup>2</sup> Dipartimento di Fisica E. Amaldi, Università degli Studi Roma Tre, via della Vasca Navale 84, 00146 Roma, Italy

<sup>3</sup> Departamento de Astrofísica, Facultad de Física, Universidad Complutense, 28040 Madrid, Spain

Received 4 February 2003 / Accepted 10 June 2003

**Abstract.** We carry out an analysis of the Mg II 2796.34 Å emission line in RS CVn stars and make a comparison with the normal stars studied in a previous paper (Paper I). The sample of RS CVn stars consists of 34 objects with known *HIPPARCOS* parallaxes and observed at high resolution with *IUE*. We confirm that RS CVn stars tend to possess wider Mg II lines than normal stars having the same absolute visual magnitude. However, we could not find any correlation between the logarithmic line width  $\log W_o$  and the absolute visual magnitude  $M_V$  (the Wilson-Bappu relationship) for these active stars, contrary to the case of normal stars addressed in Paper I. On the contrary, we find that a strong correlation exists in the ( $M_V$ ,  $\log L_{\text{Mg II}}$ ) plane ( $L_{\text{Mg II}}$  is the absolute flux in the line). In this plane, normal and RS CVn stars are distributed along two nearly parallel straight lines with RS CVn stars being systematically brighter by  $\approx 1$  dex. Such a diagram provides an interesting tool to discriminate active from normal stars. We finally analyse the distribution of RS CVn and of normal stars in the ( $\log L_{\text{Mg II}}$ ,  $\log W_o$ ) plane, and find a strong linear correlation for normal stars, which can be used for distance determinations.

**Key words.** stars: distances – stars: late-type – stars: individual: RS CVn – ultraviolet: stars – line: profiles

## 1. Introduction

The relationship between the absolute visual magnitude  $M_V$  and the width of the optical Ca II K emission line was discovered by Wilson & Bappu (1957) for stars with spectral type later than G0, and is commonly designed as the Wilson-Bappu effect (WB). This relationship has been widely studied in the optical (see Wallerstein et al. 1999, and references therein). In more recent years it has been shown that a similar relationship applies also to the Mg II k emission line at 2796.34 Å, which has the same chromospheric origin as the Ca II K line (see McClintock et al. 1975; Garcia-Alegre et al. 1981; Vladilo et al. 1987; Elgaroy et al. 1999). As for the theoretical interpretation of the Wilson-Bappu effect see Gayley (2002), the comprehensive review by Linsky (1999), and references therein. The unprecedented accuracy of the *HIPPARCOS* parallax determinations (ESA 1997) led to a substantial upgrading of the WB relationship, both in the optical (Wallerstein et al. 1999) and in the ultraviolet ranges (Scoville & Mena-Werth 1998; Elgaroy et al. 1999; Cassatella et al. 2001 – hereafter Paper I).

Active stars and, in particular, RS CVn stars were intentionally excluded in most of the above studies because of their binary nature and their enhanced chromospheric activity, but were however object of specific investigations based on the

emission doublets from Ca II (Montes et al. 1994) or Mg II (Elgarøy et al. 1997; Özeren et al. 1999). These studies lead to the definition of a WB relationship for active stars, different from that of normal stars.

In this paper we bring new observational results concerning the behaviour of the width and luminosity of the Mg II k line in RS CVn and normal stars. Our specific purposes are:

- a) to verify to which extent the observed Mg II k line width is correlated with the absolute visual magnitude for RS CVn stars, if proper account is given for their intrinsic variability;
- b) to quantify the enhancement of the chromospheric activity in RS CVn stars with respect to normal stars on the basis of the intrinsic Mg II k line luminosity;
- c) to define a Mg II k luminosity versus line width relationship for normal stars, which can be used for distance determinations.

The sample of RS CVn stars, the observations and the data reduction are presented in Sects. 2 and 3. In Sect. 4 we discuss the feasibility of defining a WB diagram for RS CVn stars. A comparison of RS CVn stars with normal stars in the Mg II luminosity versus  $M_V$  diagram is provided in Sect. 5. In Sect. 6 we present our results about the Mg II k luminosity–width correlation for normal stars and discuss the case of RS CVn stars. The conclusions are given in Sect. 7.

Send offprint requests to: A. Cassatella,  
e-mail: cassatella@fis.uniroma3.it

## 2. The present sample of stars

We have searched in the Strasbourg Data Center (SIMBAD data base) for chromospherically active binary stars of the RS CVn type for which *HIPPARCOS* parallax determinations and *IUE* long-wavelength high resolution spectra were available. The search led to a total of 55 stars. Out of these, 12 were rejected because the *IUE* data were underexposed or saturated and additional six for not fulfilling the criteria which define the RS CVn class of stars (Fekel et al. 1986; Montesinos et al. 1994): one for being a pulsating star (HIP 77512, see Fernie 1999), and five for not having been detected as variable stars by *HIPPARCOS*. Out of these latter, HIP 39348 and HIP 107095 only show micro variability, while HIP 57565, HIP 66257 and HIP 60582 are not variable according to the Variability Annex to the Catalogue. HIP 44164 (TY Pyx) was excluded in spite of being an RS CVn star because the Mg II k emission would need a dedicated analysis due to the complexity of its profile, in which the individual contribution from the components of the binary system is in general very evident. Finally, we have rejected V368 Cep and EP Eri because they are not RS CVn stars: V368 Cep has been identified as a member of the Local Association and is classified as a post T Tauri star, and EP Eri, is also a nearby young star (see Montes et al. 2001, and references therein). The final sample of RS CVn stars consists then of 34 stars.

The relevant information concerning the selected objects is given in Table 1, which provides in Cols. 1 to 4: the *HIPPARCOS* number, the star name, the spectral type and the photometric period. Columns 5 to 8 provide the  $B - V$  colour index, the parallax with its error, the absolute magnitude  $M_V$ , and the maximum amplitude of the variation in the visual band  $\Delta M_V$ . Finally, the last column specifies which component of the binary system is the active star. The relevant references to the above data are specified as footnotes to the table.

## 3. Observations and data reduction

The *IUE* high resolution long wavelength (LWP and LWR) spectra were obtained from the *INES* (IUE Newly Extracted Spectra) retrieval system through its Principal Centre at <http://ines.vilspa.esa.es>. A full description of the *INES* high resolution spectra is given in Cassatella et al. (2000), González-Riestra et al. (2000) and González-Riestra et al. (2001). The spectra were inspected individually in the Mg II 2800 Å wavelength region in order to reject noisy, overexposed or underexposed data, as in Paper I. The total number of spectra used for this investigation is 889. The Mg II k line width and flux in individual spectra were measured using the procedures described below. The results of the measurements are given in Table 2 and discussed later in detail.

Note that a considerable fraction of the observations is concentrated on a few objects and especially on V711 Tau (264 spectra), AR Lac (198 spectra),  $\lambda$  And (79 spectra), and  $\alpha$  Aur (76 spectra). The number of spectra for each star is specified in the last column of Table 2.

### 3.1. The Mg II k line width

The Mg II k line widths were determined through the procedure described in Paper I, which consists, as a first step, in defining the start and end wavelengths of the violet and red wings of the Mg II k profile and, as a second step, in fitting together the two selected regions with an unique Gaussian profile. In this way a portion of the profile can be excluded, whenever needed.

The line widths were defined as the full width of the *fitted* profile measured at half maximum of the *observed* profile.

The reason for adopting this procedure instead of measuring the line width directly on the observed line profiles, is that it allows accurate measurements to be made also in presence of noticeably asymmetric profiles, or profiles having a central depression such that the peak intensity of one of the two wings is less than 50% of the other. It is clear that, in normal stars, the central depression is essentially due to self-reversal or interstellar/circumstellar absorption.

In our specific case, however, an “absorption” dip in the profile or the presence of profile asymmetries may represent a signature of the binary nature of the object under study. A clear example of this case is the RS CVn eclipsing binary star AR Lac: the detailed study of Pagano et al. (2001) shows that the profile changes of the Mg II doublet are correlated with the orbital period so that the wavelength separation of the Mg II k emission from the K0 IV and the G2 IV components is largest at orbital quadrature, i.e. when the Doppler shift is maximum (see also Sect. 4). In order to preserve the statistical character of this investigation, no attempt will be made to fit the Mg II k line with two emission components as done for AR Lac by Pagano et al. (2001). In any case, AR Lac is, together with TY Pyx (not treated here; see Sect. 2), the only target in our sample in which the contribution from the two stars can be separated as a consequence of their similar Mg II luminosity and of the favorable inclination angle of the system.

Before performing the Gaussian fit, all spectra were re-sampled to increase the number of data points by a factor 5, and smoothed.

The errors on measured line widths were estimated to be equal to half of the sampling interval of the spectra, corresponding to  $3.64 \text{ km s}^{-1}$ . The measured line widths were corrected for instrumental broadening according the following relation:

$$W_o^2 = W^2 - b^2 \quad (1)$$

where  $W$  is the measured width,  $W_o$  the corrected value and  $b = 18 \text{ km s}^{-1}$  is the FWHM of the *IUE* Point Spread Function for high resolution spectra, assumed to be Gaussian (Evans & Imhoff 1985). The logarithm of the mean line width for each star,  $\log W_o$ , is reported in Col. 5 of Table 2. Whenever more than one spectrum was available we have reported in Col. 6 the maximum amplitude of the variations,  $\Delta \log W_o$ .

### 3.2. The Mg II k line fluxes

The Mg II k line fluxes for the RS CVn stars were obtained by direct integration of the observed profiles, as measured above the underlying local continuum. No attempt has been made

**Table 1.** Basic parameters of the RS CVn stars in the sample.

| HIP    | Name              | <i>Sp. Type</i>   | <i>P</i> (days)    | <i>B – V</i> | $\pi$ (mas)  | $M_V$ | $\Delta M_V$ | <i>Active Star</i> |
|--------|-------------------|-------------------|--------------------|--------------|--------------|-------|--------------|--------------------|
| 4157   | CF Tuc            | G0 V + K4 IV      | 2.8 <sup>2</sup>   | 0.68         | 11.60 ± 0.65 | 2.93  | 0.36         | Cool <sup>g</sup>  |
| 9630   | XX Tri            | K0 III            | 24.3 <sup>2</sup>  | 1.11         | 5.08 ± 1.10  | 1.92  | 0.36         |                    |
| 10280  | TZ Tri            | F5 + K0 III       | 14.7 <sup>2</sup>  | 0.77         | 10.68 ± 0.92 | 0.08  | 0.06         | Cool <sup>g</sup>  |
| 13118  | VY Ari            | K3-4 V–IV         | 16.6 <sup>1</sup>  | 0.96         | 22.73 ± 0.89 | 3.72  | 0.16         |                    |
| 16042  | UX Ari            | G5 V + K0 IV      | 6.4 <sup>1</sup>   | 0.88         | 19.91 ± 1.25 | 2.96  | 0.04         | Cool <sup>f</sup>  |
| 16846  | V711 Tau          | G5 V–IV + K1 IV   | 2.8 <sup>2</sup>   | 0.88         | 34.52 ± 0.86 | 3.51  | 0.09         | Both <sup>d</sup>  |
| 19431  | EI Eri            | G5 IV             | 1.9 <sup>2</sup>   | 0.71         | 17.80 ± 0.96 | 3.28  | 0.10         |                    |
| 23743  | BM Cam            | K0 III            | 80.9 <sup>1</sup>  | 1.11         | 5.22 ± 0.92  | –0.33 | 0.08         |                    |
| 24608  | $\alpha$ Aur      | G1 III + K0 III   | 8/80 <sup>2</sup>  | 0.80         | 77.29 ± 0.93 | –0.48 | 0.04         | Hot <sup>e</sup>   |
| 35600  | AR Mon            | G8 III + K2–3 III | 21.2 <sup>3</sup>  | 1.06         | 3.62 ± 1.22  | 1.52  | 0.91         | Both <sup>d</sup>  |
| 37629  | $\sigma$ Gem      | K1 III            | 19.4 <sup>2</sup>  | 1.12         | 26.68 ± 0.80 | 1.36  | 0.07         |                    |
| 46159  | IL Hya            | G8 V + K0 III–IV  | 12.8 <sup>1</sup>  | 1.01         | 8.36 ± 0.86  | 1.96  | 0.19         | Cool <sup>i</sup>  |
| 56851  | V829 Cen          | G5 V + K1 IV      | 11.7 <sup>2</sup>  | 0.95         | 8.22 ± 0.83  | 2.44  | 0.20         |                    |
| 59600  | HU Vir            | K0 III–IV         | 10.3 <sup>2</sup>  | 0.97         | 8.00 ± 1.25  | 3.21  | 0.18         |                    |
| 59796  | DK Dra            | K1 III + K1 III   | 63.0 <sup>1</sup>  | 1.15         | 7.24 ± 0.55  | 0.59  | 0.14         | Both <sup>d</sup>  |
| 64293  | RS CVn            | F4 IV + G9 IV     | 4.8 <sup>2</sup>   | 0.61         | 9.25 ± 1.06  | 2.90  | 1.27         | Cool <sup>b</sup>  |
| 65187  | BM CVn            | K1 III            | 20.6 <sup>2</sup>  | 1.16         | 9.00 ± 0.76  | 2.08  | 0.13         |                    |
| 81519  | WW Dra            | G2 IV + K0 IV     | 4.6 <sup>2</sup>   | 0.71         | 8.67 ± 1.24  | 2.92  | 0.65         | Both <sup>c</sup>  |
| 82080  | $\varepsilon$ UMi | A8–F0 V + G5 III  | 39.5 <sup>3</sup>  | 0.90         | 9.41 ± 0.67  | –0.92 | 0.06         | Cool <sup>c</sup>  |
| 84586  | V824 Ara          | G5 IV + K0 V–IV   | 1.7 <sup>2</sup>   | 0.80         | 31.83 ± 0.73 | 4.38  | 0.12         | Both <sup>e</sup>  |
| 85852  | DR Dra            | WD + K0–2 III     | 31.5 <sup>2</sup>  | 1.04         | 9.68 ± 0.80  | 1.54  | 0.06         |                    |
| 87965  | Z Her             | F4 V–IV + K0 IV   | 4.0 <sup>1</sup>   | 0.60         | 10.17 ± 0.84 | 2.28  | 0.82         | Cool <sup>b</sup>  |
| 88848  | V815 Her          | G5 V              | 1.8 <sup>2</sup>   | 0.73         | 30.69 ± 2.09 | 5.13  | 0.12         |                    |
| 94013  | V1762 Cyg         | K1 IV–III         | 28.6 <sup>2</sup>  | 1.09         | 14.24 ± 0.48 | 1.65  | 0.09         |                    |
| 95244  | V4138 Sgr         | K1 III            | 60.2 <sup>2</sup>  | 1.03         | 11.40 ± 0.86 | 2.00  | 0.17         |                    |
| 96003  | V1817 Cyg         | A2 V + K2 III–IV  | 108.8 <sup>2</sup> | 1.12         | 3.10 ± 0.50  | –1.17 | 0.06         |                    |
| 96467  | V1764 Cyg         | F–K1 III:         | 40.2 <sup>1</sup>  | 1.22         | 3.44 ± 0.90  | 0.45  | 0.16         |                    |
| 109002 | HK Lac            | F1 IV + K0 III    | 24.4 <sup>1</sup>  | 1.05         | 6.62 ± 0.61  | 1.02  | 0.22         | Cool <sup>g</sup>  |
| 109303 | AR Lac            | G2 IV + K0 IV     | 2.0 <sup>1</sup>   | 0.76         | 23.79 ± 0.59 | 2.99  | 0.74         | Both <sup>h</sup>  |
| 111072 | V350 Lac          | K2 III            | 17.7 <sup>1</sup>  | 1.17         | 8.18 ± 0.56  | 0.97  | 0.10         |                    |
| 112997 | IM Peg            | K2 III–II         | 24.4 <sup>2</sup>  | 1.13         | 10.33 ± 0.76 | 0.93  | 0.12         |                    |
| 114639 | SZ Psc            | F8 V + K1 IV      | 4.0 <sup>2</sup>   | 0.79         | 11.34 ± 0.92 | 2.67  | 0.49         | Cool <sup>c</sup>  |
| 116584 | $\lambda$ And     | G8 III–IV         | 54.3 <sup>1</sup>  | 0.98         | 38.74 ± 0.70 | 1.75  | 0.19         |                    |
| 117915 | II Peg            | K2-3 V–IV         | 6.7 <sup>1</sup>   | 1.01         | 23.62 ± 0.90 | 4.38  | 0.23         |                    |

*Notes:* spectral types are from the Catalog of Active Binary Stars (CABS) by Strassmeier et al. (1993) except for HU Vir (see Fekel et al. 1999; Montes et al. 2000). The  $B - V$  colour the parallax  $\pi$ , the absolute visual magnitude  $M_V$ , and the amplitude of its variations  $\Delta M_V$  are from the *HIPPARCOS* Catalogue and its Variability Annex.

The photometric periods  $P$  are indicated in Col. 4 together with the corresponding reference: <sup>1</sup> Variability Annex to the Hipparcos Catalogue; <sup>2</sup> CABS; <sup>3</sup> Hipparcos Input Catalogue.

For objects with double-lined spectra, the last column indicates which one of the stellar components is the active star, according to the following sources: <sup>a</sup> Gunn et al. (1998); <sup>b</sup> Fernández-Figueroa et al. (1986); <sup>c</sup> Fernández-Figueroa et al. (1994); <sup>d</sup> Montes et al. (1995a); <sup>e</sup> Montes et al. (1995b); <sup>f</sup> Montes et al. (1996); <sup>g</sup> Montes et al. (1997); <sup>h</sup> Pagano et al. (2001); <sup>i</sup> Fekel et al. (1999).

to correct the Mg II k flux for interstellar absorption since we are dealing with nearby stars and these corrections are small. Fluxes at the Earth were converted into Mg II k absolute luminosity using the parallaxes in Table 1; the logarithm of their mean values,  $\log L_{\text{Mg II}}$ , are reported in Table 2. Whenever more observations were available, the maximum amplitude of luminosity variations  $\Delta \log L_{\text{Mg II}}$  is also given.

As for the errors on the absolute line luminosity, these were derived from the errors on the parallaxes and assuming an estimated constant error of 15% on the measured fluxes.

For comparison purposes, the Mg II k flux measurements were also extended to the normal stars studied in Paper I. Their values will be used later (see Fig. 4a).

### 3.3. Absolute visual magnitudes

We have evaluated the visual magnitudes  $V_{IUE}$  from the counts of the Fine Error Sensor (FES) on board *IUE*, taken in correspondence to the spectroscopic observations.

**Table 2.** Results of the *IUE* measurements for RS CVn stars.

| HIP    | Name              | $M_V(IUE)$ | $\Delta M_V(IUE)$ | $\log W_\circ$ | $\Delta \log W_\circ$ | $\log L_{\text{Mg II}}$ | $\Delta \log L_{\text{Mg II}}$ | $N$ |
|--------|-------------------|------------|-------------------|----------------|-----------------------|-------------------------|--------------------------------|-----|
| 4157   | CF Tuc            | 2.76       | 0.17              | 2.16           | 0.15                  | 30.41                   | 0.30                           | 8   |
| 9630   | XX Tri            | 1.86       |                   | 2.07           |                       | 31.23                   |                                | 1   |
| 10280  | TZ Tri            | 0.16       | 0.05              | 2.19           | 0.02                  | 31.21                   | 0.08                           | 3   |
| 13118  | VY Ari            | 3.59       | 0.17              | 1.91           | 0.01                  | 30.13                   | 0.06                           | 5   |
| 16042  | UX Ari            | 2.89       | 0.43              | 2.09           | 0.30                  | 30.60                   | 0.53                           | 65  |
| 16846  | V711 Tau          | 3.45       | 0.46              | 2.10           | 0.48                  | 30.45                   | 0.46                           | 264 |
| 19431  | EI Eri            | 3.29       | 0.16              | 2.12           | 0.23                  | 30.23                   | 0.18                           | 28  |
| 23743  | BM Cam            | -0.32      | 0.10              | 2.23           | 0.01                  | 31.77                   | 0.08                           | 2   |
| 24608  | $\alpha$ Aur      | -0.45      | 0.22              | 2.16           | 0.23                  | 31.06                   | 0.15                           | 76  |
| 35600  | AR Mon            | 1.43       |                   | 2.41           |                       | 30.99                   |                                | 1   |
| 37629  | $\sigma$ Gem      | 1.36       | 0.26              | 2.13           | 0.30                  | 31.09                   | 0.33                           | 27  |
| 46159  | IL Hya            | 2.15       |                   | 2.02           |                       | 30.89                   |                                | 1   |
| 56851  | V829 Cen          |            |                   | 1.99           |                       | 30.67                   |                                | 1   |
| 59600  | HU Vir            | 3.25       |                   | 2.04           |                       | 30.46                   |                                | 1   |
| 59796  | DK Dra            | 0.50       | 0.14              | 2.12           | 0.13                  | 31.40                   | 0.14                           | 4   |
| 64293  | RS CVn            | 2.98       | 0.14              | 2.05           | 0.05                  | 29.96                   | 0.08                           | 3   |
| 65187  | BM CVn            |            |                   | 2.06           |                       | 30.89                   |                                | 1   |
| 81519  | WW Dra            | 3.10       |                   | 2.28           |                       | 29.97                   |                                | 1   |
| 82080  | $\varepsilon$ UMi | -0.94      | 0.00              | 2.15           | 0.10                  | 31.39                   | 0.08                           | 2   |
| 84586  | V824 Ara          | 4.30       | 0.07              | 2.13           | 0.05                  | 30.05                   | 0.33                           | 3   |
| 85852  | DR Dra            | 1.62       |                   | 2.05           |                       | 30.88                   |                                | 1   |
| 87965  | Z Her             | 2.29       |                   | 1.82           |                       | 29.92                   |                                | 1   |
| 88848  | V815 Her          | 5.10       | 0.05              | 1.87           | 0.16                  | 29.33                   | 0.10                           | 4   |
| 94013  | V1762 Cyg         | 1.76       | 0.19              | 2.09           | 0.04                  | 30.98                   | 0.06                           | 4   |
| 95244  | V4138 Sgr         | 2.17       |                   | 1.92           |                       | 30.76                   |                                | 1   |
| 96003  | V1817 Cyg         | -1.23      |                   | 2.22           |                       | 32.11                   |                                | 1   |
| 96467  | V1764 Cyg         | 0.35       |                   | 2.34           |                       | 31.53                   |                                | 1   |
| 109002 | HK Lac            | 1.03       | 0.13              | 2.14           | 0.07                  | 31.36                   | 0.20                           | 4   |
| 109303 | AR Lac            | 3.08       | 0.90              | 2.28           | 0.33                  | 30.19                   | 0.47                           | 198 |
| 111072 | V350 Lac          | 1.03       | 0.05              | 2.16           | 0.09                  | 30.97                   | 0.11                           | 2   |
| 112997 | IM Peg            | 0.94       | 0.22              | 2.15           | 0.17                  | 31.34                   | 0.20                           | 12  |
| 114639 | SZ Psc            | 2.64       | 0.33              | 2.22           | 0.17                  | 30.54                   | 0.23                           | 25  |
| 116584 | $\lambda$ And     | 1.75       | 0.35              | 2.01           | 0.22                  | 30.90                   | 0.33                           | 79  |
| 117915 | II Peg            | 4.33       | 0.44              | 1.94           | 0.33                  | 30.07                   | 0.45                           | 59  |

*Notes:*  $M_V(IUE)$  and  $\Delta M_V(IUE)$  are the mean visual absolute magnitude and its maximum amplitude.  $\log W_\circ$  and  $\Delta \log W_\circ$  are, respectively, the logarithm of the mean full-width at half-maximum for the Mg II line and the corresponding spread.  $\log L_{\text{Mg II}}$  and  $\Delta \log L_{\text{Mg II}}$  are, respectively, the logarithm of the mean luminosity of the Mg II line and its spread.  $N$  is the number of the spectra used for each star. Units for the line widths  $W_\circ$  and Mg II luminosities are in  $\text{km s}^{-1}$  and  $\text{erg s}^{-1}$ , respectively.

The procedure used to obtain the FES visual magnitudes consists in correcting the FES counts for the dead time and for the time-dependent sensitivity degradation, in converting the corrected counts into FES magnitudes, and in reporting them into the Johnson photometric system through the application of a colour correction which depends on the star's colour index  $B - V$ .

Several FES calibrations have been published during the *IUE* lifetime. They mainly differ for the way the FES time-dependent degradation is corrected for (see Barylak et al. 1985; Imhoff & Wasatonic 1986; Fireman & Imhoff 1989; Pérez & Loomis 1991; Pérez 1992). For the observations obtained

before 1990, we adopted the correction algorithm suggested by Pérez & Loomis (1991), which is based on an accurate analysis of a very large number of observations. For dates after 1990 (date of the change of the FES reference point), we used the algorithm by Pérez (1992).

The absolute magnitudes were computed from the *HIPPARCOS* trigonometric parallaxes without any allowance for interstellar reddening. The corresponding errors were derived from the errors on the trigonometric parallaxes and assuming a typical error of  $\pm 0.01$  mag on the visual magnitudes from the *HIPPARCOS* Catalogue, and  $\pm 0.05$  mag for  $V_{IUE}$  as suggested by Pérez & Loomis (1991).

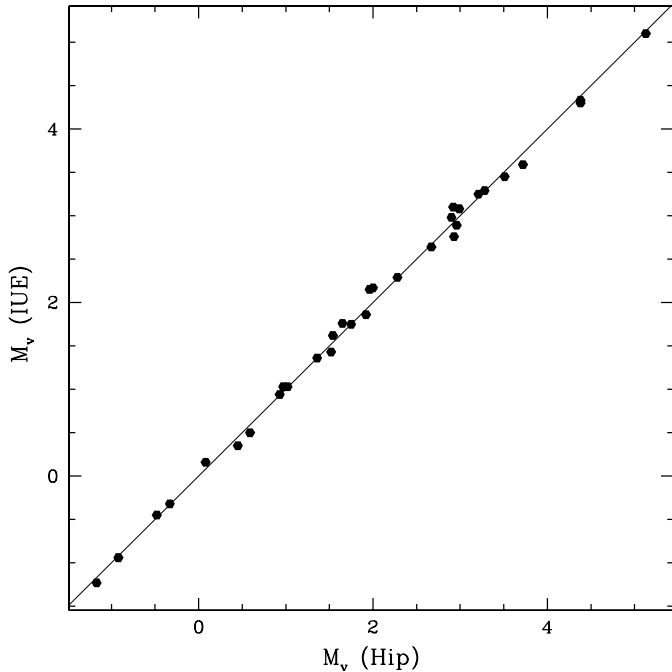


**Fig. 1.** The mean absolute visual magnitude derived from the *IUE* FES counts,  $M_V(IUE)$ , is plotted against the *HIPPARCOS* absolute visual magnitude  $M_V$  for the stars in Tables 1 and 2. The figure shows that there are no systematic errors when using *IUE* magnitudes over the wide range of values covered.

The mean values of the absolute magnitudes  $M_V(IUE)$  for the RS CVn stars in our sample and the maximum amplitude of the variations  $\Delta M_V(IUE)$  are reported in Table 2, except for HIP 56851 and HIP 65187 (no FES observations were available).

We note that the amplitudes of the photometric variations  $\Delta M_V(IUE)$  do not coincide exactly with the corresponding values from the *HIPPARCOS* Catalogue (cf. Cols. 8 and 4 of Tables 1 and 2, respectively). This is due to the considerably longer time span covered by the *HIPPARCOS* observations and to the different kind of monitoring.

In Fig. 1 we show a comparison of the absolute visual magnitudes obtained from the FES counts and the corresponding *HIPPARCOS* values. The two sets of data agree to within 0.08 mag (rms). Since this value is only slightly larger than the expected error on  $V_{IUE}$ , and given the statistical nature of this paper, we will use as a default the *HIPPARCOS* values, without any significant loss of accuracy. The  $M_V(IUE)$  values will be used only in the specific case of AR Lac, discussed in the next section.

#### 4. The WB diagram for RS CVn stars

As mentioned in the Introduction, the Wilson-Bappu effect in active stars has been studied by Montes et al. (1994), Elgarøy et al. (1997), and Özeren et al. (1999). These authors found that active stars, and RS CVn stars in particular, have substantially broader lines than normal stars and that, in spite of the large spread, the line widths are well correlated with the visual absolute magnitudes ( $r = 0.80$  to  $0.93$ ). We wish to stress that in

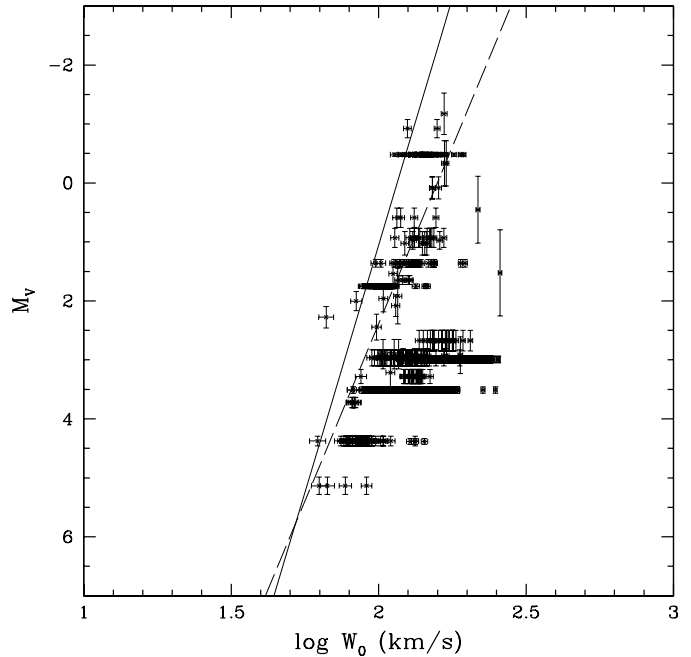


**Fig. 2.** The Wilson-Bappu effect in the Mg II k line for RS CVn stars. Overlaid to the data points we show the WB relationship for normal stars from Paper I (full line), and for RS CVn stars (dashed line) from Özeren et al. (1999).

all the above analyses, the mean values for the line widths were used instead of the individual determinations.

On the other hand, we believe that the variety of orbital and structural parameters in these binary systems should have important effects on the observed line widths. For this reason we have decided to use *all* good quality *IUE* spectra available for each of the stars in our sample.

Our results concerning the Wilson-Bappu effect in RS CVn stars are shown in Fig. 2, where the absolute magnitude  $M_V$  is plotted as a function of  $\log W_0$ . The figure reports the individual measurements together with the corresponding error bars and indicates, for reference, the regression line describing the Wilson-Bappu effect for normal stars from Paper I (full line)

$$M_V = (34.56 \pm 0.29) - (16.75 \pm 0.14) \log W_0. \quad (2)$$

where  $W_0$  is in  $\text{km s}^{-1}$ .

In Fig. 2 we also indicate, as a dashed line, the magnitude-width linear relationship for RS CVn stars by Özeren et al. (1999). We cannot make a direct comparison with other studies because they are based on a different line (Ca II; see Montes et al. 1994), or make use of a different definition of the Mg II line width (Elgarøy et al. 1997).

Figure 2 shows that RS CVn stars have in general broader lines than normal stars, as also found by the previously quoted authors. It also shows, however, that the magnitude-width relationship by Özeren et al. (1999) does not provide a good representation for the stars in our sample. This is not surprising, since  $M_V$  and  $\log W_0$  in our data set are clearly uncorrelated: the correlation coefficient for these individual determinations is indeed as low as  $r = 0.17$ . A major cause for the above discrepancy and for the lack of correlation is most likely the intrinsic

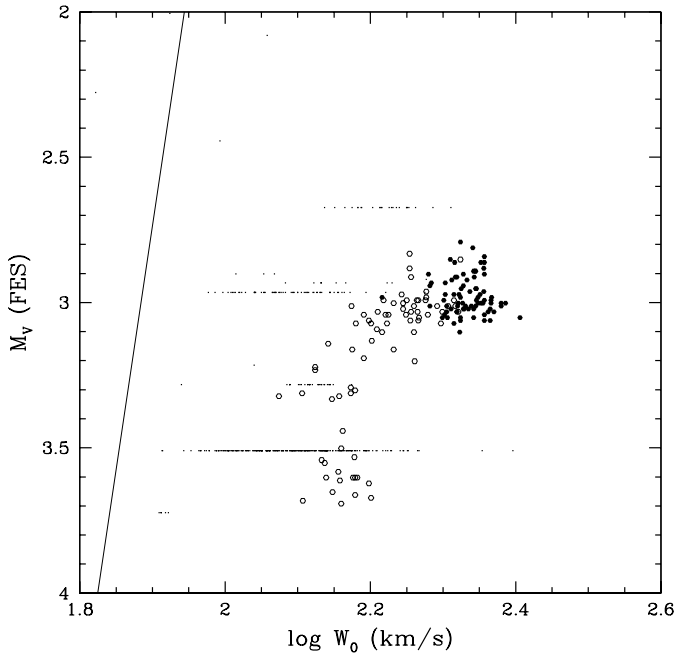


**Fig. 3.** The Wilson-Bappu effect in a restricted range of coordinate's values to show the large variations of AR Lac (circles). Filled circles correspond to data close to quadrature (see text). The straight line represents the relationship for normal stars described in Paper I (see Eq. (2)). Dots represent the other RS CVn stars.

variability and the variety of orbital and structural parameters in these binary systems.

To underline the influence of orbital motion we consider the case of AR Lac, which is the second best monitored RS CVn star, with a total of 198 *IUE* observations along 15 years. AR Lac is a G2 IV + K0 IV eclipsing binary system, whose components are spin-orbit coupled with a 1.98 day period (see Pagano et al. 2001 and references therein). Given the quite large amplitude of variability for this object (both in  $M_V$  and in  $\log W_0$ , see Table 2) we have in this special case computed the absolute magnitudes from the FES counts obtained at the moment of the spectroscopic observations and from the *HIPPARCOS* parallax (see Sect. 3.3). A magnification of the WB diagram, centered around AR Lac is shown in Fig. 3, without the error bars. This star, indicated with filled and open circles, describes half a loop in the diagram, with a considerable excursion in both axes. To understand this behaviour we have indicated with filled circles the data obtained at phases  $\phi$  near quadrature ( $0.12 \leq \phi \leq 0.37$  and  $0.62 \leq \phi \leq 0.88$ ). It is immediately clear that these phases are characterized by the broadest Mg II line profiles and the highest luminosity levels, which is just what is expected considering the eclipsing binary nature of AR Lac and the similar  $V$  magnitudes and spectral types of the components of the system.

AR Lac is a limiting case. More in general, our data indicate that whenever a star has been observed frequently, the fluctuations in line width  $\Delta \log W_0$  may be quite large (10% to 20%, see Table 2).

In conclusion, it is not possible with the present data to define a WB relationship for RS CVn stars because of the

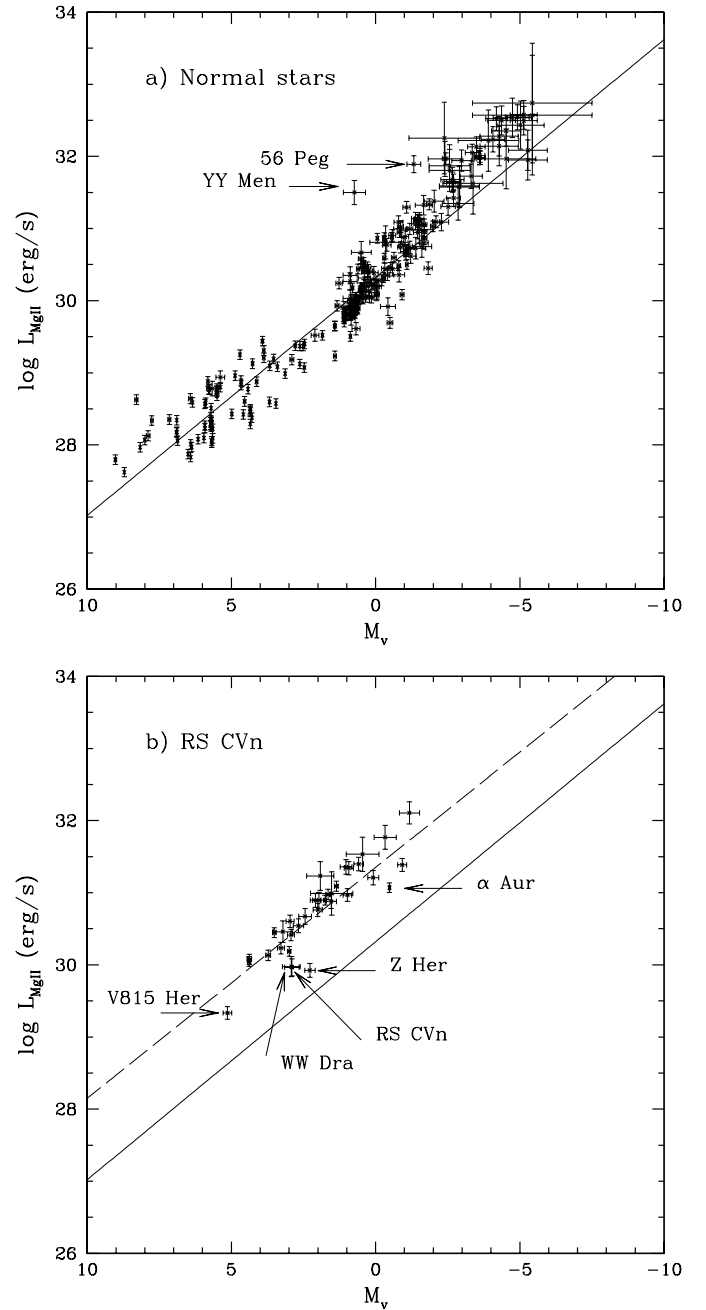


**Fig. 4.** The logarithmic absolute luminosity in the Mg II k line is plotted as a function of the absolute visual magnitude. **a)** Normal stars. The individual measurements with the corresponding error bars are indicated. The straight line is the linear fit to the data (Eq. (3)). **b)** RS CVn stars. The mean values and the corresponding error bars are reported. We indicate also the linear fits to the RS CVn data (dashed line; see Eq. (4)) and to the normal stars data (full line).

impossibility to disentangle the effects of stellar activity from orbital effects.

## 5. The Mg II luminosity vs. $M_V$ relationship

As shown by several authors (see e.g. Basri 1987; Cerruti-Sola et al. 1992; Elgaroy et al. 1997), the Mg II k flux is a strong indicator of stellar activity. In this section we consider

the Mg II k absolute line luminosity  $L_{\text{Mg II}}$  as an indicator of the enhanced activity level of RS CVn stars compared with normal stars (see Paper I).

The absolute Mg II k luminosities were obtained from the observed fluxes as described in Sect. 3.2.

### 5.1. Normal stars

In Fig. 4a we show the  $\log L_{\text{Mg II}}$  vs.  $M_V$  diagram for normal stars. A linear fit to the data, performed by taking into account the observational errors on both variables, provides:

$$\log L_{\text{Mg II}} = (30.32 \pm 0.01) - (0.33 \pm 0.01) M_V \quad (3)$$

where  $L_{\text{Mg II}}$  is in  $\text{erg s}^{-1}$ . In spite of the wide range of luminosity covered, the correlation index is very good ( $r = 0.96$ ).

A similar relationship has been obtained by Weiler & Oegerle (1979) from OAO 3 moderate-resolution (0.51 Å) observations of 73 late-type stars. The difference in the coefficients might be ascribed to the different resolution and accuracy level of the two space experiments or, more likely, to the mixture of quiet and active stars in their sample.

It is worth noticing that two stars, 56 Peg and YY Men, indicated with arrows in Fig. 4a, which appear significantly brighter in the Mg II line than predicted on the basis of the above relationship, are peculiar stars that were erroneously included in our sample of Paper I. In particular, 56 Peg is a G8 Ib barium star, reported by Cornide et al. (1992) as the most active of the sample of 10 barium stars they studied in the Ca II line. YY Men is a K1 IIIp star belonging to the FK Com class, as defined by Bopp & Stencel (1981). As evolved late-type stars, the enhanced chromospheric activity level denoted by the strength of the Mg II k line is likely linked to the fact that both stars are fast rotators (the rotational period of YY Men is 9.5476 days according to Cutispoto et al. 1992).

### 5.2. RS CVn stars

In Fig. 4b we show the  $\log L_{\text{Mg II}}$  versus  $M_V$  diagram for RS CVn stars and, for comparison, the regression line applicable to normal stars (full line; Eq. (3)).

To find an analytical representation to the data of RS CVn stars in Fig. 4b, one is faced with the difficulty posed by the very sparse distribution of the observations (see Table 2), which would in fact lead to overweighting the few most frequently observed stars. For this reason we have considered appropriate to perform a fit using the mean values for the individual stars, weighted according to the observational errors (i.e. the fixed 15% percent error on the Mg II k fluxes, and the parallax error; see Sect. 3.2).

A linear fit to the data provides:

$$\log L_{\text{Mg II}} = (31.35 \pm 0.03) - (0.32 \pm 0.01) M_V. \quad (4)$$

The fit is indicated as a dashed line in the above figure. The corresponding correlation coefficient is  $r = 0.90$ , to be compared with  $r = 0.82$  if the individual measurements are taken into account. The Mg II k line luminosity appears then to be strongly correlated with  $M_V$  (Eq. (4)), contrary to the Mg II line width (Sect. 4).

When comparing the linear fits of RS CVn stars with that of normal stars we notice the following important properties:

- a) RS CVn stars are systematically brighter by  $\approx 1$  dex in the Mg II k line than normal stars. This produces a sort of luminosity gap (at a given  $M_V$ ) between normal and RS CVn stars;
- b) the slope of the two straight lines is the same within the errors.

There are five objects that appear to be somewhat less luminous than expected in the Mg II k line: RS CVn, Z Her, WW Dra, V815 Her, and  $\alpha$  Aur. Their positions are indicated with arrows in the  $(L_{\text{Mg II}}, M_V)$  plane of Fig. 4. The former three have a common peculiarity: the star that mainly contributes to the Mg II k emission flux is the cool component, while the residual flux at the bottom of the broad Mg II photospheric absorption is mainly due to the hotter component. Stars with these characteristics were not included in the sample of RS CVn stars by Montes et al. (1994).

As for  $\alpha$  Aur, it cannot be considered as a typical RS CVn star because, contrary to what generally observed in this class of stars, the hotter component is more active than the cool one because it is a faster rotator. In the case of the other deviating star, V815 Her, its cool component is probably an M1–2 V star according to CABS. If this is correct, the object would better qualify as a BY Dra star.

The diagrams in Fig. 4 have a practical diagnostics application: if the distance to a star is known (in addition to its visual magnitude and Mg II k flux) one can easily distinguish a quiet star from an active star such as RS CVn's.

## 6. The Mg II k absolute luminosity vs. width relationship

In this section we look for a correlation between the absolute luminosity in the Mg II line and the corresponding line width for the sample of normal stars in Paper I and, separately, for the present sample of RS CVn stars.

### 6.1. Normal stars

We have performed a linear fit to the  $\log L_{\text{Mg II}}$  and  $\log W_\circ$  data for normal stars. Taking the observational errors into account we find:

$$\log L_{\text{Mg II}} = (16.40 \pm 0.15) + (6.81 \pm 0.07) \log W_\circ. \quad (5)$$

where the errors on the coefficients represent the confidence level of the regression line. The correlation coefficient is  $r = 0.9$ . We note that the above coefficients are close, but not identical, to those obtained by combining Eqs. (2) and (3). This is an expected consequence of the correlation coefficient not being unity.

In Fig. 5a we plot the  $\log L_{\text{Mg II}}$  and  $\log W_\circ$  data together with the above linear relationship. We observe that the corresponding correlation coefficient is fairly high in spite of the  $\approx 6$  orders of magnitude span in line luminosity. This is a remarkable result in itself, which should deserve proper study for its implications in the understanding of line broadening mechanisms in the chromospheres of stars.

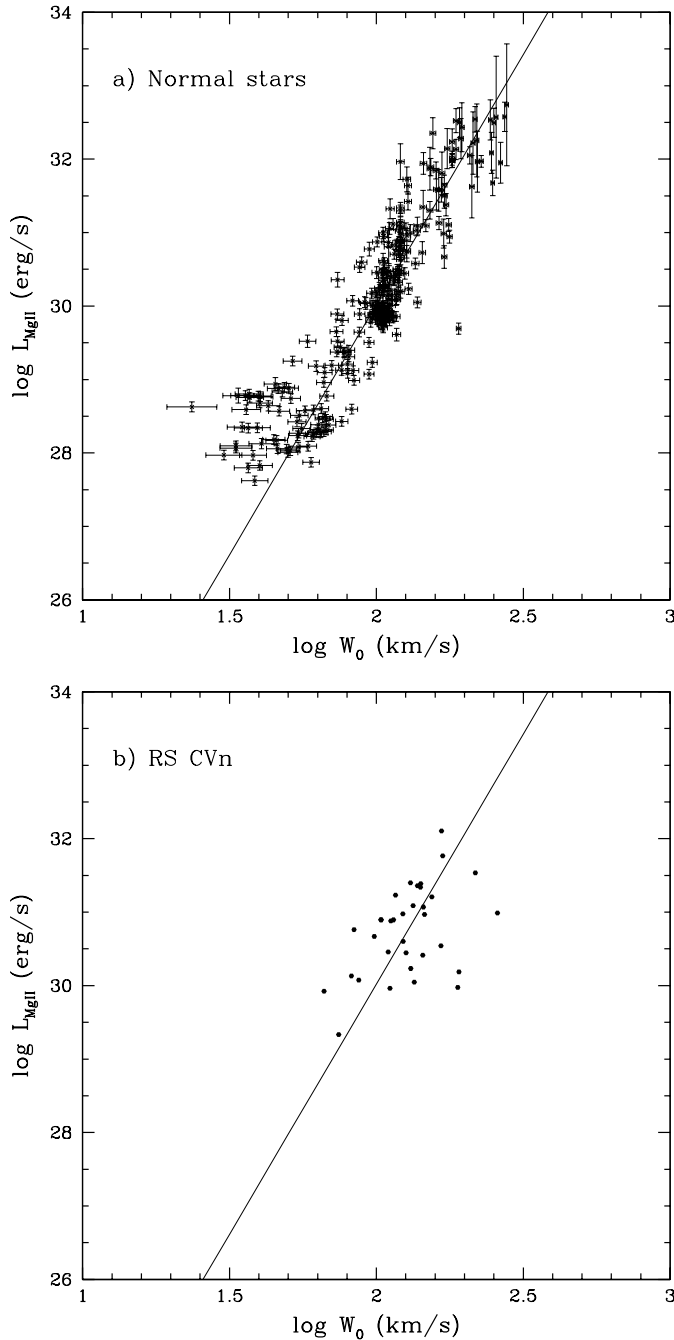


**Fig. 5.** The absolute luminosity in the Mg II k line as a function of line width. Panel **a**) gives the results for the sample of normal stars in Paper I, together with the linear fit in Eq. (5). Panel **b**) gives the results for the RS CVn stars in Table 1 and shows, for comparison, the above linear fit for normal stars.

Another interesting aspect of Eq. (5) is that it allows a quite reliable distance determination to be made using spectrophotometric data only. The distance to the star is readily obtained by comparing the observed Mg II k flux with the absolute Mg II k luminosity corresponding, via Eq. (5), to the observed value of  $\log W_0$ . If proper account is taken for the spread of the data points about the regression line, the standard error on the distance determinations is about 32%, to be compared with a

value of about 25% if the distances are obtained via the WB relationship in Eq. (2).

This small difference in accuracy is probably due to the higher accuracy of optical photometry compared to *IUE* photometry. We conclude that Eq. (5) represents an interesting alternative to the classical Wilson-Bappu effect.

## 6.2. RS CVn stars

Based on the data reported in Table 2, we plot in Fig. 5b, on a logarithmic scale, the mean Mg II k absolute luminosity as a function of the mean line width for the RS CVn stars in our sample.

It clearly appears from the figure that the range of coordinate values covered by RS CVn stars is quite narrow. More importantly, the correlation index corresponding to these data is extremely low:  $r = 0.05$  for individual measurements, and  $r = 0.47$  for the mean values. This prevents one to attempting any analytical representation to the data.

We then conclude that, at the present stage, the Mg II k line cannot be used to determine the distance of RS CVn stars.

## 7. Conclusions and discussion

This paper is based on the analysis of the Mg II k emission line width and flux in 34 RS CVn stars and 230 normal stars observed by *IUE* at high resolution, for which *HIPPARCOS* parallax determinations were available. The number of spectra used is very large: 889 and 303, for the two classes, respectively.

Our results can be summarized as follows:

- The distribution of RS CVn stars in the  $(\log W_0, M_V)$  plane does not show any regular pattern, as reflected by the very low correlation index between these variables. Therefore, no Wilson-Bappu relationship could be found for such stars, contrary to the case of normal stars studied in Paper I. The absence of such a correlation is due to their intrinsic variability and to the wide spread of orbital and structural parameters of these binary systems (see Sect. 4).
- On the contrary, RS CVn stars are closely correlated in the  $(M_V, \log L_{\text{Mg II}})$  plane, where they are well represented by a straight line (Eq. (4)). Such a strong correlation is also found for normal stars, which lie along a nearly parallel line (Eq. (3)), but are systematically fainter in the Mg II k line by a factor of  $\approx 10$  compared to RS CVn stars (Figs. 4a, b). These properties should provide interesting constraints on the modeling of RS CVn chromospheres and represent a reliable tool to discriminate between normal and RS CVn stars, at least in the range of  $M_V$  covered ( $\approx 5$  to  $-2$ ).
- The data for normal stars are strongly correlated in the  $(\log W_0, \log L_{\text{Mg II}})$  plane (see Fig. 5a), allowing the linear relationship in Eq. (5) to be defined. This equation represents an interesting alternative to the standard Wilson-Bappu method for distance determinations, it offers nearly the same accuracy, is based only on spectrophotometric data of the Mg II line, and is applicable to stars covering  $\approx 6$  orders of magnitude in line luminosity.



On the contrary, no similar correlation has been found for RS CVn stars (Fig. 5b).

*Acknowledgements.* The authors are grateful to Prof. J. Linsky for stimulating suggestions and to Dr. D. Marinucci for useful comments.

## References

- Barylak, M., Wasatonic, R., & Imhoff, C. L. 1985, NASA IUE Newslett., 26, 101
- Bopp, B. W., & Stencel, R. E. 1981, AJ, 247, 131
- Cassatella, A., Altamore, A., González-Riestra, R., et al. 2000, A&AS, 141, 331
- Basri, G. 1987, ApJ, 316, 377
- Cassatella, A., Altamore, A., Badiali, M., & Cardini, D. 2001, A&A, 374, 1085
- Cerruti-Sola, M., Cheng, C.-C., & Pallavicini, R. 1992, A&A, 256, 185
- Cornide, M., Fernández-Figueroa, M. J., De Castro, E., & Armentia, J. 1992, AJ, 103, 1374
- Cutispoto, G., Pagano, I., & Rodonó, M. 1992, A&A, 263, L3
- Elgarøy, Ø., Engvold, O., & Lund, N. 1999, A&A, 343, 222
- Elgarøy, Ø., Engvold, O., & Jorås, P. 1997, A&A, 326, 165
- ESA 1997, The Hypparcos and Tycho Catalogues, ESA SP-1200
- Evans, N. R., & Imhoff, C. L. 1985, NASA IUE Newslett., 28, 77
- Fekel, F. C., Moffet, T. J., & Henry, G. W. 1986, ApJS, 60, 551
- Fekel, F. C., Strassmeier, K. G., Weber, M., & Washúttl, A. 1999, A&AS, 137, 369
- Fernández-Figueroa, M. J., Montes, D., De Castro, E., & Cornide, M. 1994, ApJS, 90, 433
- Fernández-Figueroa, M. J., Montesinos, B., De Castro, E., et al. 1986, A&A, 169, 219
- Fernie, J. D. 1999, IBVS, 4473
- Fireman, G. F., & Imhoff, C. L. 1989, NASA IUE Newslett., 40, 10
- Garcia-Alegre, M. C., Ponz, J. D., & Vásquez, M. 1981, A&A, 96, 17
- Gayley, K. G. 2002, ApJ, 565, 545
- Gunn, A. G., Mitrou, C. K., & Doyle, J. G. 1998, MNRAS, 296, 150
- González-Riestra, R., Cassatella, A., Solano, E., Altamore, A., & Wamsteker, W. 2000, A&AS, 141, 343
- González-Riestra, R., Cassatella, A., & Wamsteker, W. 2001, A&A, 373, 730
- Imhoff, C. L., & Wasatonic, R. 1986, NASA IUE Newslett., 29, 45
- Linsky, J. L. 1999, ApJ, 525, 776
- McClintock, W., Linsky, J. L., Henry, R. C., & Moos, H. W. 1975, ApJ, 202, 733
- Montes, D., Fernández-Figueroa, M. J., De Castro, E., & Cornide, M. 1994, A&A, 285, 609
- Montes, D., Fernández-Figueroa, M. J., De Castro, E., & Cornide, M. 1995a, A&AS, 109, 135
- Montes, D., De Castro, E., Fernández-Figueroa, M. J., & Cornide, M. 1995b, A&AS, 114, 287
- Montes, D., Sanz-Forcada, J., Fernández-Figueroa, M. J., & Lorente, R. 1996, A&A, 310, L27
- Montes, D., Fernández-Figueroa, M. J., De Castro, E., & Sanz-Forcada, J. 1997, A&AS, 125, 263
- Montes, D., Fernández-Figueroa, M. J., De Castro, E., et al. 2000, A&A, 146, 103
- Montes, D., López-Santiago, J., Fernández-Figueroa, M. J., & Galvez, M. C. 2001, A&A, 379, 976
- Montesinos, B., Gimenez, A., & Fernández-Figueroa, M. J. 1994, MNRAS, 232, 361
- Özeren, F. F., Doyle, J. G., & Jevremovic, D. 1999, A&A, 350, 635
- Pagano, I., Rodonó, M., Linsky, J. L., et al. 2001, A&A, 365, 128
- Pérez, M., & Loomis, C. 1991, Report to the Three Agency Meeting, F-13
- Pérez, M. 1992, NASA IUE Newslett., 48, 76
- Scoville, F., & Mena-Werth, J. 1998, PASP, 110, 794
- Strassmeier, K. G., Rice, C. B., Fekel, F. C., & Scheck, M. 1993, A&AS, 100, 173
- Vladilo, G., Molaro, P., Crivellari, L., et al. 1987, A&A, 185, 233
- Wallerstein, G., Machado-Pelaez, L., & Gonzalez, G. 1999, PASP, 111, 335
- Weiler, E. J., & Oegerle, W. R. 1979, ApJS, 39, 537
- Wilson, O. C., & Bappu, M. K. V. 1957, ApJ, 125, 661